

Higher-Order DGFEM Transport Calculations on Polytope Meshes for Massively-Parallel Architectures

Michael W. Hackemack

Chair: Jean C. Ragusa

Committee Members: Marvin L. Adams, Jim E. Morel, Nancy M. Amato

External Advisor: Troy Becker

Department of Nuclear Engineering
Texas A&M University
College Station, TX, USA 77843
mike.hack@tamu.edu



Outline

1 Overview

- The DGFEM S_N Transport Equation
- Polytope Grid Motivation

2 Polytope Finite Element Basis Functions

- Linear Basis Functions on 2D Polygons
- Quadratic Serendipity Basis Functions on 2D Polygons
- Linear Basis Functions on 3D Polyhedra

3 Diffusion Synthetic Acceleration on Polytopes

- Theory
- MIP Diffusion Form

4 Proposed Work and Current Status

5 Ongoing Work

The Continuous-Energy Transport Equation

Transport Equation

$$[\Omega \cdot \nabla + \sigma_t(\mathbf{r}, E)] \psi(\mathbf{r}, E, \Omega) = \int_{4\pi} \int_0^\infty \sigma_s(\mathbf{r}, E', E, \Omega', \Omega) \psi(\mathbf{r}, E', \Omega') dE' d\Omega' + Q(\mathbf{r}, E, \Omega)$$

Boundary Conditions

$$\psi(\mathbf{r}, E, \Omega) = \psi^{inc}(\mathbf{r}, E, \Omega) + \int_{4\pi} \int_0^\infty \beta(\mathbf{r}, E', E, \Omega', \Omega) \psi(\mathbf{r}, E', \Omega') dE' d\Omega'$$

Term Definitions

\mathbf{r} - neutron position

E - neutron energy

Ω - neutron solid angle

$\psi(\mathbf{r}, E, \Omega)$ - angular flux

$Q(\mathbf{r}, E, \Omega)$ - distributed neutron source

$\sigma_t(\mathbf{r}, E)$ - total macroscopic cross section

$\sigma_s(\mathbf{r}, E', E, \Omega', \Omega)$ - total macroscopic scattering cross section

$\beta(\mathbf{r}, E', E, \Omega', \Omega)$ - boundary albedo

Energy and Angular Discretization

The multigroup S_N equations

$$(\mathbf{\Omega}_m \cdot \nabla + \sigma_{t,g}) \psi_{m,g} = \sum_{g'=1}^G \sum_{p=0}^{N_p} \frac{2p+1}{4\pi} \sigma_{s,p}^{g' \rightarrow g} \sum_{n=-p}^p \phi_{p,n,g'} Y_{p,n}(\mathbf{\Omega}_m) + Q_{m,g}$$

Multigroup Method

$$\psi_g = \int_{E_g}^{E_{g-1}} \psi(E) dE$$

S_N Discretization

$$\phi_{p,n} \equiv \int_{4\pi} d\Omega \psi(\mathbf{\Omega}) Y_{p,n}(\mathbf{\Omega}),$$

$$\sigma_{s,p} \equiv \int_{-1}^1 d\mu \sigma_s(\mu_0) P_p(\mu_0)$$

$$\mu_0 \equiv \mathbf{\Omega}' \cdot \mathbf{\Omega}$$

$$\sigma_s(\mathbf{\Omega}' \cdot \mathbf{\Omega}) \equiv \frac{1}{2\pi} \sigma_s(\mu)$$

$$P_p(\mathbf{\Omega}' \cdot \mathbf{\Omega}) \equiv \frac{1}{2\pi} P_p(\mu)$$

Spatial Discretization

Iterative Procedure

Classic Source Iteration

$$\Psi^{(\ell+1)} = \mathbf{L}^{-1} \left(\mathbf{M} \Sigma \Phi^{(\ell)} + \mathbf{Q} \right)$$

$$\Phi^{(\ell+1)} = \mathbf{D} \mathbf{L}^{-1} \left(\mathbf{M} \Sigma \Phi^{(\ell)} + \mathbf{Q} \right)$$

$$\Phi = \mathbf{D} \Psi$$

Operator Terms

\mathbf{L} - streaming + collision operator

\mathbf{M} - moment-to-discrete operator

\mathbf{D} - discrete-to-moment operator

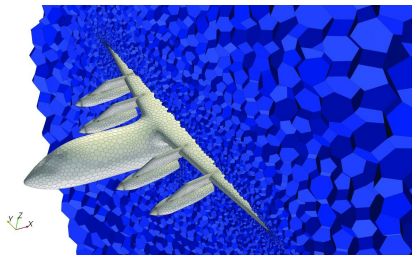
Σ - scattering operator

Transport Sweep

The operation \mathbf{L}^{-1} can be performed in myriad ways. For this work, we will use the matrix-free, full-domain transport sweep.

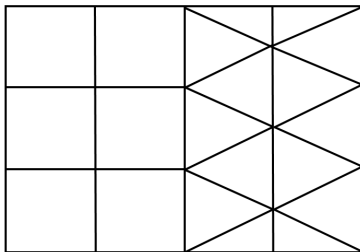
Polytope Grid Motivation

- Other physics communities are now employing polytope grids due to decreased cell/face counts (CFD in particular)
- They allow for transition elements between different domain regions
- Hanging nodes from non-conforming meshes are not necessary
- Independently-generated simplicial grids (*i.e.* created in parallel) can be stitched together with polytopes without communicating the whole mesh across processors



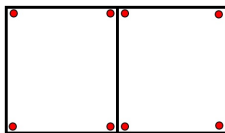
Polytope Grid Motivation

- Other physics communities are now employing polytope grids due to decreased cell/face counts (CFD in particular)
- They allow for transition elements between different domain regions
- Hanging nodes from non-conforming meshes are not necessary
- Independently-generated simplicial grids (*i.e.* created in parallel) can be stitched together with polytopes without communicating the whole mesh across processors

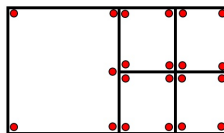


Polytope Grid Motivation

- Other physics communities are now employing polytope grids due to decreased cell/face counts (CFD in particular)
- They allow for transition elements between different domain regions
- Hanging nodes from non-conforming meshes are not necessary
- Independently-generated simplicial grids (*i.e.* created in parallel) can be stitched together with polytopes without communicating the whole mesh across processors



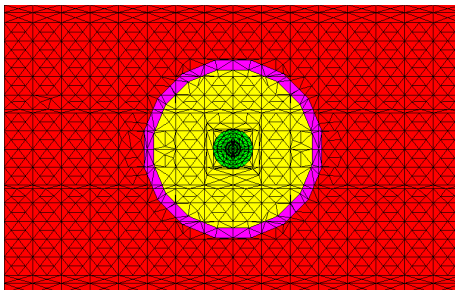
(a)



(b)

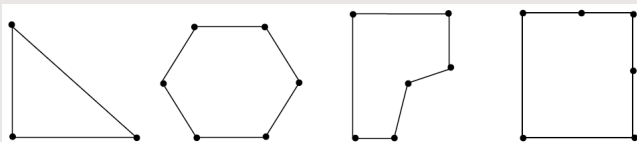
Polytope Grid Motivation

- Other physics communities are now employing polytope grids due to decreased cell/face counts (CFD in particular)
- They allow for transition elements between different domain regions
- Hanging nodes from non-conforming meshes are not necessary
- Independently-generated simplicial grids (*i.e.* created in parallel) can be stitched together with polytopes without communicating the whole mesh across processors

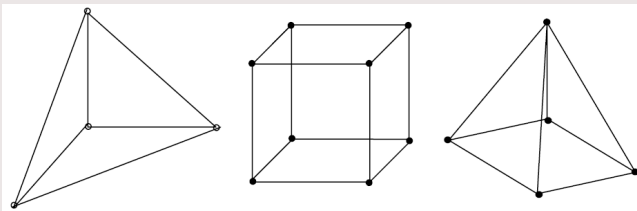


Polytope Finite Elements

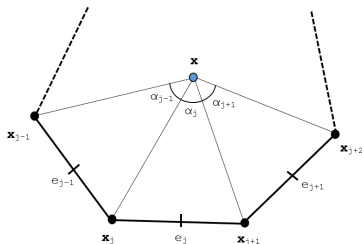
2D arbitrary convex/concave polygons



3D convex polyhedra



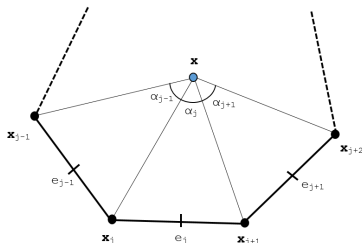
Linear Basis Functions on 2D Polygons



Basis Function Properties - Barycentric Coordinates

- 1 $\lambda_i \geq 0$
- 2 $\sum_i \lambda_i = 1$
- 3 $\sum_i \mathbf{x}_i \lambda_i(\mathbf{x}) = \mathbf{x}$
- 4 $\lambda_i(\mathbf{x}_j) = \delta_{ij}$

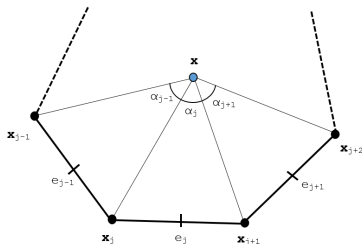
Wachspress Rational Functions



$$\lambda_i^w(\mathbf{x}) = \frac{w_i(\mathbf{x})}{\sum_j w_j(\mathbf{x})}, \quad w_j(\mathbf{x}) = \frac{A(\mathbf{x}_{j-1}, \mathbf{x}_j, \mathbf{x}_{j+1})}{A(\mathbf{x}, \mathbf{x}_{j-1}, \mathbf{x}_j) A(\mathbf{x}, \mathbf{x}_j, \mathbf{x}_{j+1})}$$

$$A(\mathbf{x}_1, \mathbf{x}_2, \mathbf{x}_3) = \frac{1}{2} \begin{vmatrix} 1 & 1 & 1 \\ x_1 & x_2 & x_3 \\ y_1 & y_2 & y_3 \end{vmatrix}$$

Piecewise Linear (PWL) Functions



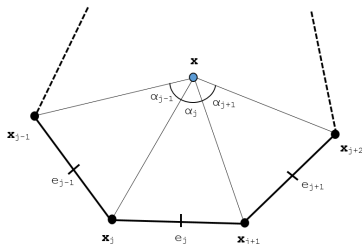
$$\lambda_i^{PWL}(\mathbf{x}) = t_i(\mathbf{x}) + \alpha_i t_c(\mathbf{x})$$

t_i - standard 2D linear function; 1 at vertex i that linearly decreases to 0 to the cell center and the adjoining vertices

t_c - 2D tent function; 1 at cell center and linearly decreases to 0 to each cell vertex

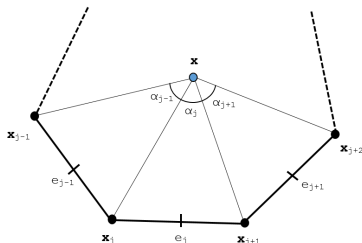
$\alpha_i = \frac{1}{N_V}$ - weight parameter for vertex i

Mean Value Coordinates



$$\lambda_i^{MV}(\mathbf{x}) = \frac{w_i(\mathbf{x})}{\sum_j w_j(\mathbf{x})}, \quad w_j(\mathbf{x}) = \frac{\tan(\alpha_{j-1}/2) + \tan(\alpha_j/2)}{|\mathbf{x}_j - \mathbf{x}|}$$

Maximum Entropy Coordinates



$$\lambda_i^{ME}(\mathbf{x}) = \frac{w_i(\mathbf{x})}{\sum_j w_j(\mathbf{x})}, \quad w_j(\mathbf{x}) = m_j(\mathbf{x}) \exp(-\omega^* \cdot (\mathbf{x}_j - \mathbf{x}))$$

$$\omega^* = \operatorname{argmin} F(\omega, \mathbf{x}) \quad F(\omega, \mathbf{x}) = \ln \left(\sum_j w_j(\mathbf{x}) \right)$$

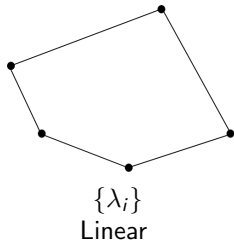
Summary of the 2D Linear Basis Functions

Basis Function	Dimension	Polytope Types	Analytical/Numerical	Direct/Iterative
Wachspress	2D/3D	Convex*	Numerical	Direct
PWL	1D/2D/3D	Convex/Concave	Analytical	Direct
Mean Value	2D**	Convex/Concave	Numerical	Direct
Max Entropy	1D/2D/3D	Convex/Concave	Numerical	Iterative***

- * - weak convexity for Wachspress coordinates does not cause blow up
- ** - mean value 3D analogue only applicable to tetrahedron
- *** - maximum entropy minimization solved via Newton's Method

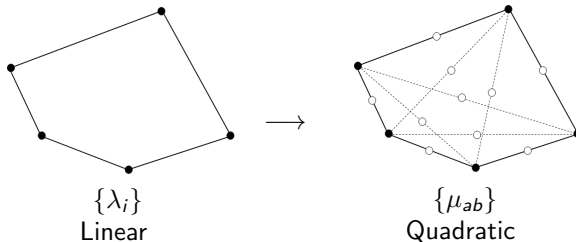
Quadratic Serendipity Basis Functions on 2D Polygons

- 1 Form the linear barycentric functions - $\{\lambda_i\}$
- 2 Construct the pairwise products - $\{\mu_{ab}\}$
- 3 Eliminate the interior nodes to form a serendipity basis - $\{\xi_{ij}\}$



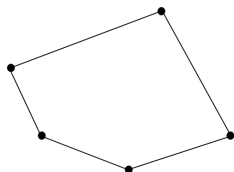
Quadratic Serendipity Basis Functions on 2D Polygons

- 1 Form the linear barycentric functions - $\{\lambda_i\}$
- 2 Construct the pairwise products - $\{\mu_{ab}\}$
- 3 Eliminate the interior nodes to form a serendipity basis - $\{\xi_{ij}\}$

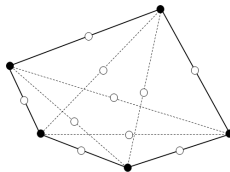


Quadratic Serendipity Basis Functions on 2D Polygons

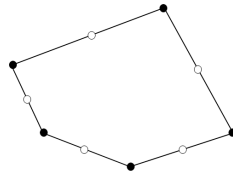
- 1 Form the linear barycentric functions - $\{\lambda_i\}$
- 2 Construct the pairwise products - $\{\mu_{ab}\}$
- 3 Eliminate the interior nodes to form a serendipity basis - $\{\xi_{ij}\}$



$\{\lambda_i\}$
Linear



$\{\mu_{ab}\}$
Quadratic



$\{\xi_{ij}\}$
Serendipity

Pairwise products of the barycentric basis functions

Necessary Precision Properties

$$\sum_{aa \in V} \mu_{aa} + \sum_{ab \in E \cup D} 2\mu_{ab} = 1$$

$$\sum_{aa \in V} \mathbf{x}_{aa} \mu_{aa} + \sum_{ab \in E \cup D} 2\mathbf{x}_{ab} \mu_{ab} = \mathbf{x}$$

$$\sum_{aa \in V} \mathbf{x}_a \mathbf{x}_a^T \mu_{aa} + \sum_{ab \in E \cup D} (\mathbf{x}_a \mathbf{x}_b^T + \mathbf{x}_b \mathbf{x}_a^T) \mu_{ab} = \mathbf{xx}^T$$

Further Notation/Notes

$$\mathbf{x}_{ab} = \frac{\mathbf{x}_a + \mathbf{x}_b}{2}, \quad \mu_{ab} = \lambda_a \lambda_b$$

$$\mu_{ab}^K(\mathbf{r}) = 0, \quad \{ab \in D, \mathbf{r} \in \partial K\}$$

Eliminate interior nodes to form serendipity basis

Reduction Problem - $[\xi] := \mathbb{A} [\mu]$

$$\mathbb{A} = \begin{bmatrix} c_{11}^{11} & \dots & c_{ab}^{11} & \dots & c_{(n-2)n}^{11} \\ \dots & \ddots & \vdots & \ddots & \vdots \\ c_{11}^{ij} & \dots & c_{ab}^{ij} & \dots & c_{(n-2)n}^{ij} \\ \dots & \ddots & \vdots & \ddots & \vdots \\ c_{11}^{n(n+1)} & \dots & c_{ab}^{n(n+1)} & \dots & c_{(n-2)n}^{n(n+1)} \end{bmatrix}$$

Serendipity Precision Properties

$$\sum_{ii \in V} \xi_{ii} + \sum_{i(i+1) \in E} 2\xi_{i(i+1)} = 1$$

$$\sum_{ii \in V} \mathbf{x}_{ii} \xi_{ii} + \sum_{i(i+1) \in E} 2\mathbf{x}_{i(i+1)} \xi_{i(i+1)} = \mathbf{x}$$

$$\sum_{ii \in V} \mathbf{x}_i \mathbf{x}_i^T \xi_{ii} + \sum_{i(i+1) \in E} \left(\mathbf{x}_i \mathbf{x}_{i+1}^T + \mathbf{x}_{i+1} \mathbf{x}_i^T \right) \xi_{i(i+1)} = \mathbf{x} \mathbf{x}^T$$

Special case - bilinear coordinates on the unit square

Bilinear coordinates and quadratic extension

$$\lambda_1 = (1-x)(1-y)$$

$$\lambda_2 = x(1-y)$$

$$\lambda_3 = xy$$

$$\lambda_4 = (1-x)y$$

$$\mu_{11} = (1-x)^2(1-y)^2 \quad \mu_{12} = (1-x)x(1-y)^2$$

$$\mu_{22} = x^2(1-y)^2 \quad \mu_{23} = x^2y(1-y)$$

$$\mu_{33} = x^2y^2 \quad \mu_{34} = (1-x)xy^2$$

$$\mu_{44} = (1-x)^2y^2 \quad \mu_{41} = (1-x)^2y(1-y)$$

$$\mu_{13} = (1-x)x(1-y)y \quad \mu_{24} = (1-x)x(1-y)y$$

Reduction matrix

$$\mathbb{A} = \begin{bmatrix} 1 & 0 & 0 & 0 & 0 & 0 & 0 & 0 & -1 & 0 \\ 0 & 1 & 0 & 0 & 0 & 0 & 0 & 0 & 0 & -1 \\ 0 & 0 & 1 & 0 & 0 & 0 & 0 & 0 & -1 & 0 \\ 0 & 0 & 0 & 1 & 0 & 0 & 0 & 0 & 0 & -1 \\ 0 & 0 & 0 & 0 & 1 & 0 & 0 & 0 & 1/2 & 1/2 \\ 0 & 0 & 0 & 0 & 0 & 1 & 0 & 0 & 1/2 & 1/2 \\ 0 & 0 & 0 & 0 & 0 & 0 & 1 & 0 & 1/2 & 1/2 \\ 0 & 0 & 0 & 0 & 0 & 0 & 0 & 1 & 1/2 & 1/2 \end{bmatrix}$$

Serendipity coordinates

$$\xi_{11} = (1-x)(1-y)(1-x-y)$$

$$\xi_{22} = x(1-y)(x-y)$$

$$\xi_{33} = xy(-1+x+y)$$

$$\xi_{44} = (1-x)y(y-x)$$

$$\xi_{12} = (1-x)x(1-y)$$

$$\xi_{23} = xy(1-y)$$

$$\xi_{34} = (1-x)xy$$

$$\xi_{41} = (1-x)y(1-y)$$

Linear Basis Functions on 3D Polyhedra

Linear basis functions and convex polyhedra only for 3D

- The 2D quadratic serendipity formulation is more arduous in 3D
- Intercell coupling is not straightforward for concave polyhedra
- Focus on 3D PWL functions - MAXENT only other function for arbitrary polyhedra
- Focus on 3D parallelepipeds and extruded convex polygons (convex prisms)

3D PWL basis functions

$$b_i(\mathbf{x}) = t_i(\mathbf{x}) + \sum_{f=1}^{F_i} \beta_f^i t_f(\mathbf{x}) + \alpha_i t_c(\mathbf{x})$$

t_i - standard 3D linear function; 1 at vertex i , linearly decreases to 0 to the cell center, each adjoining face center, and each adjoining vertex

t_c - 3D tent function; 1 at cell center, linearly decreases to 0

t_f - face tent function; 1 at face center, linearly decreases to 0 at each face vertex and cell center

$\alpha_i = \frac{1}{N_V}$ - weight parameter for vertex i

$\beta_f^i = \frac{1}{N_f}$ - weight parameter for face f touching vertex i

Theory goes here...

Theory goes here...

The diffusion equation is used as our low-order operator

The Diffusion Equation

$$-\nabla \cdot D \nabla \Phi(\mathbf{r}) + \sigma \Phi(\mathbf{r}) = q(\mathbf{r}), \quad \mathbf{r} \in \mathcal{D}$$

General Boundary Conditions

$$\begin{aligned} \Phi(\mathbf{r}) &= \Phi_0(\mathbf{r}), & \mathbf{r} \in \partial \mathcal{D}^d \\ -D \partial_n \Phi(\mathbf{r}) &= J_0(\mathbf{r}), & \mathbf{r} \in \partial \mathcal{D}^n \\ \frac{1}{4} \Phi(\mathbf{r}) + \frac{1}{2} D \partial_n \Phi(\mathbf{r}) &= J^{inc}(\mathbf{r}), & \mathbf{r} \in \partial \mathcal{D}^r \end{aligned}$$

Desirable diffusion form properties

- Can handle concave and degenerate polytope cells
- Symmetric Positive-Definite (SPD)
- Availability of suitable preconditioners
- Agnostic of directionality of interior faces

Symmetric Interior Penalty (SIP) Form

Bilinear Form

$$\begin{aligned}
 a(\Phi, b) = & \left\langle D\nabla\Phi, \nabla b \right\rangle_{\mathcal{D}} + \left\langle \sigma\Phi, b \right\rangle_{\mathcal{D}} \\
 & + \left\{ \kappa_e^{SIP} [[\Phi], [b]] \right\}_{E_h^i} - \left\{ [[\Phi], \{ \{ D\partial_n b \} \}] \right\}_{E_h^i} - \left\{ \{ \{ D\partial_n \Phi \} \}, [[b]] \right\}_{E_h^i} \\
 & + \left\{ \kappa_e^{SIP} \Phi, b \right\}_{\partial\mathcal{D}^d} - \left\{ \Phi, D\partial_n b \right\}_{\partial\mathcal{D}^d} - \left\{ D\partial_n \Phi, b \right\}_{\partial\mathcal{D}^d} + \frac{1}{2} \left\{ \Phi, b \right\}_{\partial\mathcal{D}^r}
 \end{aligned}$$

Linear Form

$$\begin{aligned}
 \ell(b) = & \left\langle q, b \right\rangle_{\mathcal{D}} - \left\{ J_0, b \right\}_{\partial\mathcal{D}^n} + 2 \left\{ J_{inc}, b \right\}_{\partial\mathcal{D}^r} \\
 & + \left\{ \kappa_e^{SIP} \Phi_0, b \right\}_{\partial\mathcal{D}^d} - \left\{ \Phi_0, D\partial_n b \right\}_{\partial\mathcal{D}^d}
 \end{aligned}$$

SIP Penalty Coefficient

$$\kappa_e^{SIP} \equiv \begin{cases} \frac{C_B}{2} \left(\frac{D^+}{h^+} + \frac{D^-}{h^-} \right) & , e \in E_h^i \\ C_B \frac{D^-}{h^-} & , e \in \partial\mathcal{D} \end{cases}$$

$$C_B = cp(p+1)$$

c - user defined constant ($c \geq 1$)

p - polynomial order of the finite element basis (1, 2, 3, ...)

$D^{(+/-)}$ - diffusion coefficient defined on the positive/negative side of a face

$h^{(+/-)}$ - orthogonal projection defined on the positive/negative side of a face

$$u^\pm = \lim_{s \rightarrow 0^\pm} u(\mathbf{r} + s\mathbf{n})$$

Modified Interior Penalty (MIP) Form

Diffusion Form

$$\begin{aligned}
& \langle D \nabla \Phi, \nabla b \rangle_{\mathcal{D}} + \langle \sigma \Phi, b \rangle_{\mathcal{D}} \\
& + \left\{ \kappa_e^{MIP} \llbracket \Phi \rrbracket, \llbracket b \rrbracket \right\}_{E_h^i} - \left\{ \llbracket \Phi \rrbracket, \{ \{ D \partial_n b \} \} \right\}_{E_h^i} - \left\{ \{ \{ D \partial_n \Phi \} \}, \llbracket b \rrbracket \right\}_{E_h^i} \\
& + \left\{ \kappa_e^{MIP} \Phi, b \right\}_{\partial \mathcal{D}^{vac}} - \frac{1}{2} \left\{ \Phi, D \partial_n b \right\}_{\partial \mathcal{D}^{vac}} - \frac{1}{2} \left\{ D \partial_n \Phi, b \right\}_{\partial \mathcal{D}^{vac}} \\
& = \langle q, b \rangle_{\mathcal{D}}
\end{aligned}$$

MIP Penalty Term

$$\kappa_e^{MIP} = \max\left(\frac{1}{4}, \kappa_e^{SIP}\right)$$

Proposed Work

POLYFEM

- 1 Analyze the different 2D linear polygonal basis functions for use in DGFEM transport calculations
- 2 Perform the same analysis with the quadratic serendipity basis functions

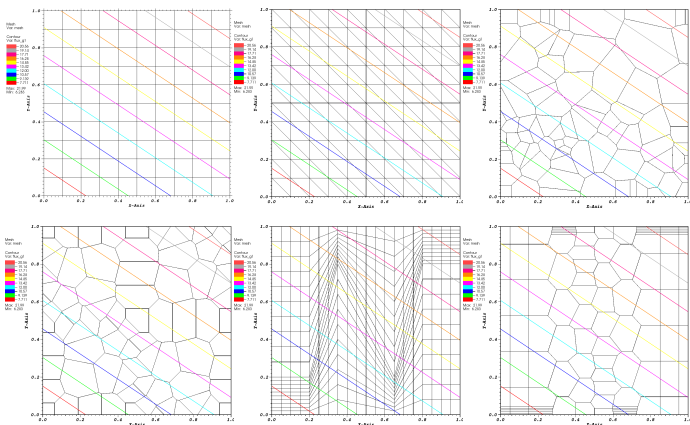
MIP DSA

- 1 Analyze the 2D linear/quadratic basis functions with DSA preconditioning through Fourier/numerical analysis
- 2 Extend the analysis of MIP DSA to arbitrary convex 3D polyhedra
- 3 Implement MIP DSA in PDT using HYPRE
 - 1 Analyze the scalability of the method to high process counts
 - 2 Perform parametric studies on aggregation/partitioning factors to generate a performance model of MIP DSA with HYPRE
 - 3 Implement and perform analysis of two-grid acceleration at scale
 - 4 Run real-world numerical experiments - IM1

2D Exactly-Linear Transport Solutions - mean value coordinates

$$\mu \frac{\partial \psi}{\partial x} + \eta \frac{\partial \psi}{\partial y} + \sigma_t \psi = Q(x, y, \mu, \eta)$$

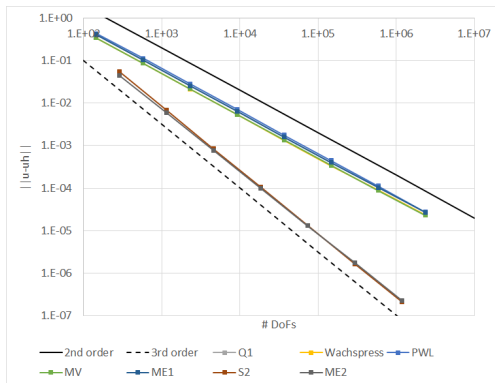
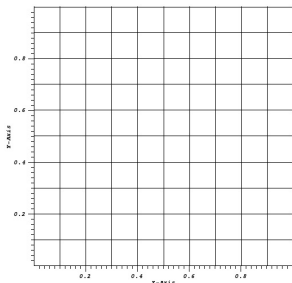
$$\psi(x, y, \mu, \eta) = ax + by + c\mu + d\eta + e, \quad \phi(x, y) = 2\pi(ax + by + e)$$



Convergence rates using MMS for the 2D polygonal basis functions

$$\psi(x, y) = \sin\left(\nu \frac{\pi x}{L_x}\right) \sin\left(\nu \frac{\pi y}{L_y}\right)$$

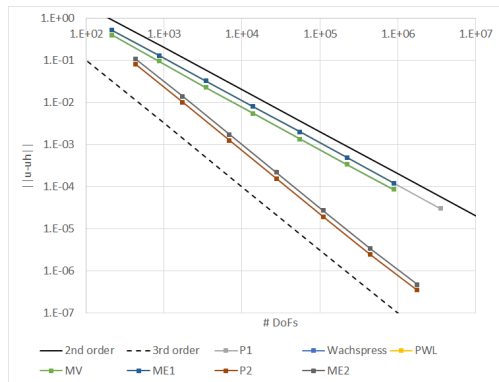
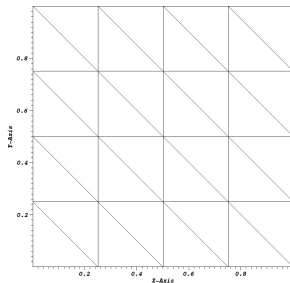
$$\phi(x, y) = 2\pi \sin\left(\nu \frac{\pi x}{L_x}\right) \sin\left(\nu \frac{\pi y}{L_y}\right)$$



Convergence rates using MMS for the 2D polygonal basis functions

$$\psi(x, y) = \sin\left(\nu \frac{\pi x}{L_x}\right) \sin\left(\nu \frac{\pi y}{L_y}\right)$$

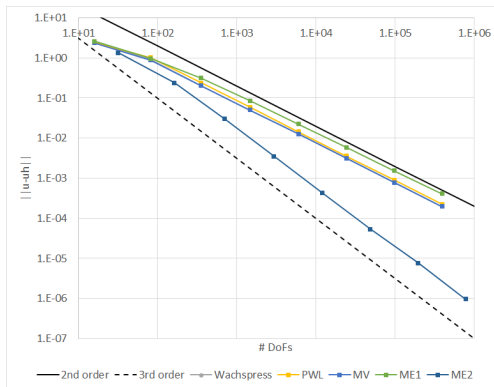
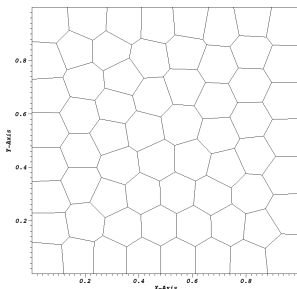
$$\phi(x, y) = 2\pi \sin\left(\nu \frac{\pi x}{L_x}\right) \sin\left(\nu \frac{\pi y}{L_y}\right)$$



Convergence rates using MMS for the 2D polygonal basis functions

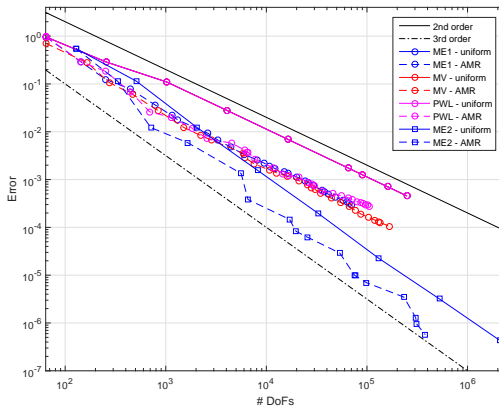
$$\psi(x, y) = \sin\left(\nu \frac{\pi x}{L_x}\right) \sin\left(\nu \frac{\pi y}{L_y}\right)$$

$$\phi(x, y) = 2\pi \sin\left(\nu \frac{\pi x}{L_x}\right) \sin\left(\nu \frac{\pi y}{L_y}\right)$$

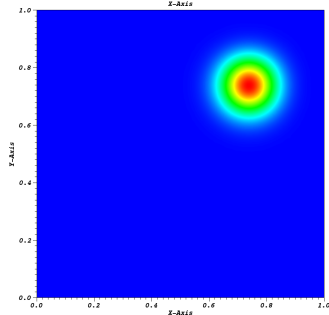
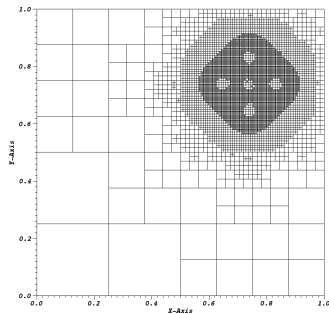
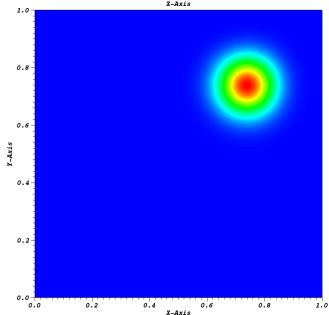
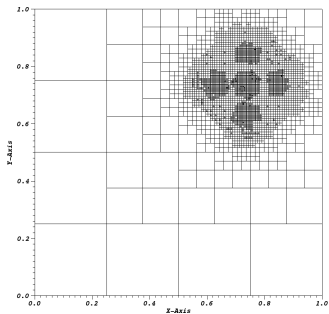


Convergence rates using MMS and AMR for the 2D polygonal basis functions

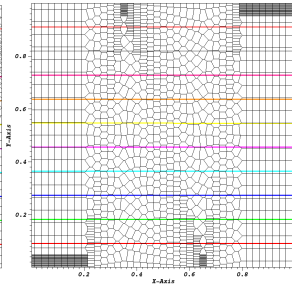
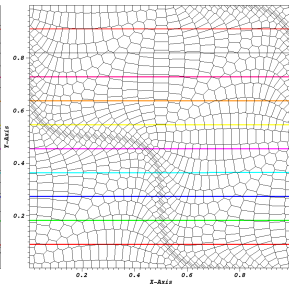
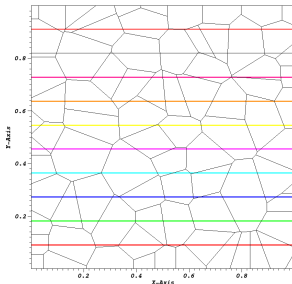
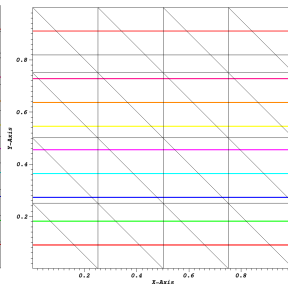
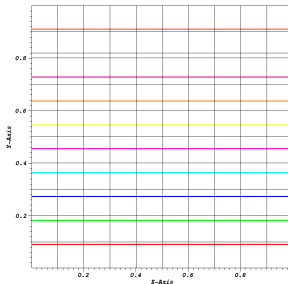
$$\psi(x, y) = x(L_x - x)y(L_y - y) \exp\left(-\frac{(x - x_0)^2 + (y - y_0)^2}{\gamma}\right),$$
$$\phi(x, y) = 2\pi x(L_x - x)y(L_y - y) \exp\left(-\frac{(x - x_0)^2 + (y - y_0)^2}{\gamma}\right)$$



Linear ME cycle 15 (left) and quadratic ME cycle 08 (right)

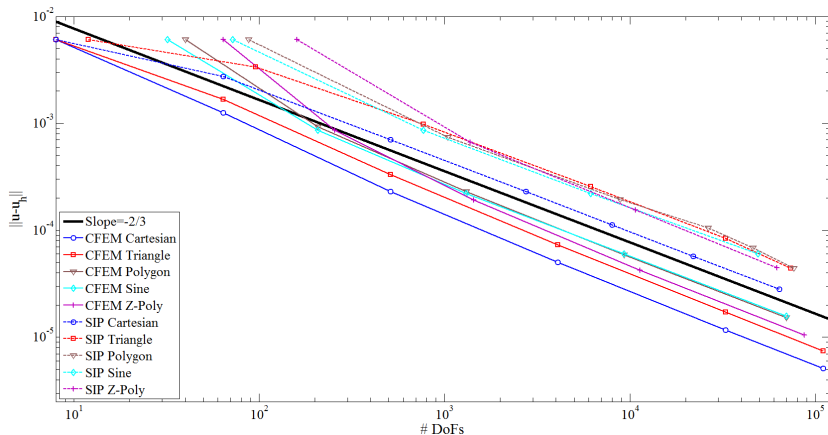


SIP exactly linear solutions on 3D polyhedral meshes using the PWL basis functions



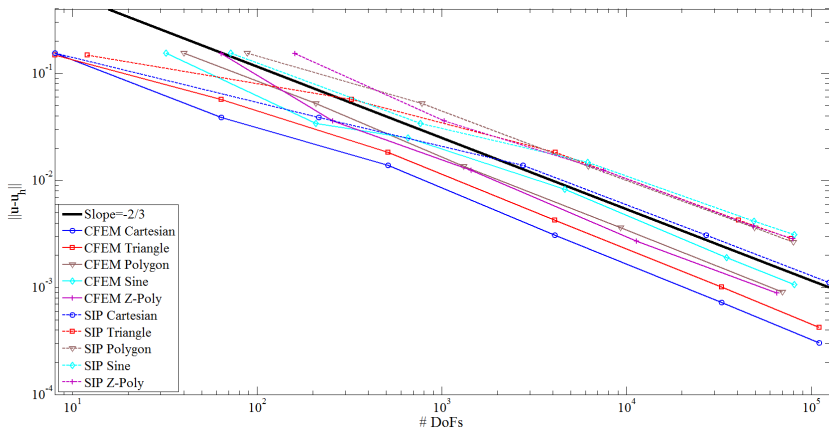
SIP convergence study - quadratic solution on 3D cube using the PWL basis functions

$$\Phi(x, y, z) = xyz(L_x - x)(L_y - y)(L_z - z)$$
$$L_x = L_y = L_z = 1.0$$

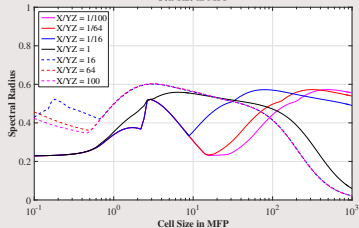
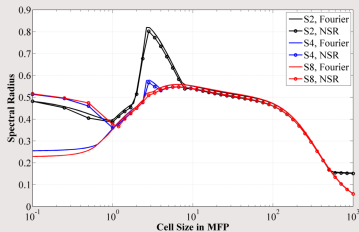
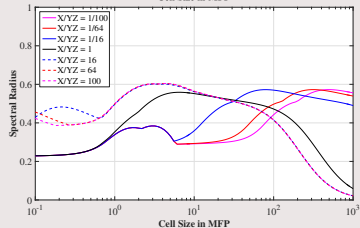
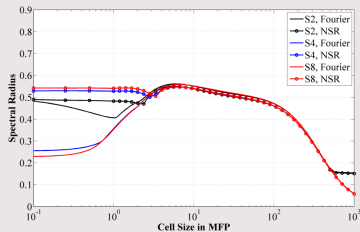


SIP convergence study - gaussian solution on 3D cube using the PWL basis functions

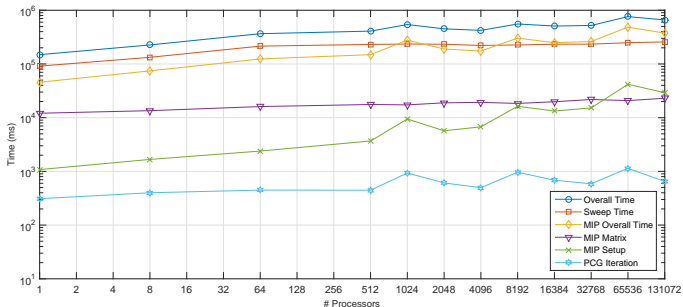
$$\Phi(x, y, z) = xyz(L_x - x)(L_y - y)(L_z - z) \exp(-(\mathbf{r} - \mathbf{r}_0) \cdot (\mathbf{r} - \mathbf{r}_0))$$
$$L_x = L_y = L_z = 1.0, \quad \mathbf{r}_0 = (3/4, 3/4, 3/4)$$



Fourier analysis - 3D PWL basis functions

 $c = 1$  $c = 4$ 

MIP DSA Timing Data with PDT on Vulcan using HYPRE



Problem Description

- Modified Zerr problem - used optimal sweep aggregation parameters
 - homogeneous cube - about 500 mfp and $c=0.9999$
 - S8 level-symmetric quadrature
- pointwise convergence tolerance of $1e-8$
- SI precondition with MIP DSA using HYPRE PCG and AMG

Two-grid acceleration implementation in PDT

- Successfully implemented and debugged
 - Includes non-orthogonal mesh configurations
 - Includes multi-material configurations
- Have tested the two-grid methodology on a homogeneous graphite block as well as a block with an air duct
- Iteration counts for a very large configuration (very optically thick) are similar to simple infinite medium calculations

Materials	Unaccelerated Iterations	Accelerated Iterations
Graphite Only	2027	21
Graphite + Air Duct	2138	23

POLYFEM Ongoing Work

- Finish quadratic serendipity extension for polygonal finite elements to Wachspress, PWL, and mean value.
- Determine the effects of numerical integration strategies on highly-distorted polygonal elements
- Perform analysis on benchmark cases using AMR
 - Searchlight problem (partially completed)
 - IAEA-EIR-2 problem

MIP DSA Ongoing Work

- Finish the MIP DSA Fourier analysis for all the 2D polygonal basis functions (including the quadratic serendipity extension).
- Analyze the effects of AMR with polygonal basis functions on the MIP DSA PCG iteration counts (with and without bootstrapping)
- Remaining PDT work:
 - Complete parametric studies (a lot of the raw results have been compiled) of MIP DSA with HYPRE and generate a working performance model
 - Perform additional two-grid acceleration studies on simple geometries
 - Run IM1 problem with two-grid acceleration
 - Commit all acceleration additions to master for use in the CERT project

Questions?

A special acknowledgment to the Department of Energy Rickover Fellowship Program in Nuclear Engineering, which provides strong support to its fellows and their professional development.



TEXAS A&M 
ENGINEERING

